

Effects on Stacking Fault Energies in Austenitic Stainless Steels



X. W. Zhou¹, C. Nowak¹, R. S. Skelton¹, M. E. Foster¹, J. A. Ronevich¹, C. San Marchi¹, and R. B. Sills²

¹Sandia National Laboratories, USA; ²Rutgers University, USA

2021 MRS Fall Meeting, Virtual, Dec 6 - Dec 8, 2021

Sandia National Laboratories is a multi-mission laboratory managed and operated by National Technology and Engineering Solutions of Sandia, LLC., a wholly owned subsidiary of Honeywell International, Inc., for the U.S. Department of Energy's National Nuclear Security Administration under contract DE-NA-0003525. The views expressed in the article do not necessarily represent the views of the U.S. Department of Energy or the United States Government.

Sandia National Laboratories is a multi-mission laboratory managed and operated by National Technology & Engineering Solutions of Sandia, LLC, a wholly owned subsidiary of Honeywell International Inc., for the U.S. Department of Energy's National Nuclear Security Administration under contract DE-NA0003525.

Stacking Fault Energy (SFE) on Hydrogen Embrittlement

- SFE is related to hydrogen compatibility parameter RRA (relative reduction in area) in JOM, 72, 1982 (2020):
 - RRA > 80% when SFE > 40 mJ/m²;
 - RRA ~ 20-80% when SFE ~ 20-40 mJ/m².
- The austenitic stainless steels (e.g., 304L) deform through hydrogen-mediated slip bands in Metall. Mater. Trans. A, 52, 1516 (2021).
- We have performed a detailed study on SFE using molecular dynamics (MD). This has also led to an Fe-Ni-Cr-H potential.

Presentation Outline

- An Fe-Ni-Cr-H interatomic potential
- Experimental validation of molecular dynamics (MD) simulations
- Stacking fault energy calculations

The presented work has been published in Inter. J. Hydrogen Energy.

Adding H to an Existing Fe-Ni-Cr

Potential

- No Fe-Ni-Cr-H potential is available in literature, but H can be added to an existing Fe-Ni-Cr potential.
- Smith and Was' potential (PRB 1989, 40, 10322) was fitted to effective atoms and did not consider SFE (stacking fault energy), not chosen.
- The 2013 Bonny et al's potential (MSMSE 2013, 21, 085004) predicts phase separation, not chosen.
- The 2011 Bonny et al's potential (MSMSE 2011, 19, 085008) predicts negative slope of SFE with Ni composition (should be positive), not chosen.
- Tong et al's potential (Mol. Sim. 2016, 42, 1256) predicts large negative stacking fault energy, not chosen.
- The 2018 Bonny et al's potential (MSMSE, 2018, 26, 065014) is based on the 2013 version, not chosen.
- We adopted our Fe-Ni-Cr potential (J. Comp. Chem., 2018, 39, 2420).
- Other potentials (e.g., by Mendelev et al) are also available more recently, but are not tested.

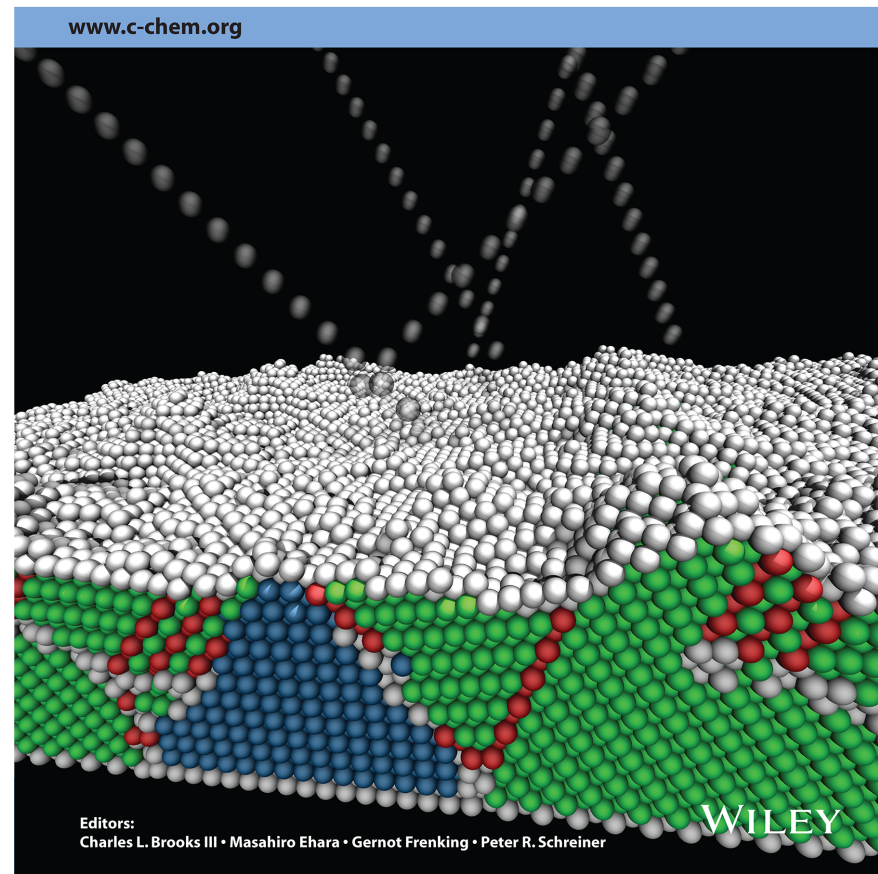
Our Fe-Ni-Cr-H Potential

- Energy, volume, stability trends in Fe, Ni, Cr.
- Lattice / elastic constants, and SFE in Fe, Ni, Cr.
- H swelling volume in Fe, Ni, Cr.
- H diffusion energy barriers in Fe, Ni, Cr.
- H-vacancy and H-interstitial energies in Fe, N, Cr.
- H trapping energies in Fe, Ni, Cr.

Zhou et al, J. Comp. Chem., 39, 2420 (2018).

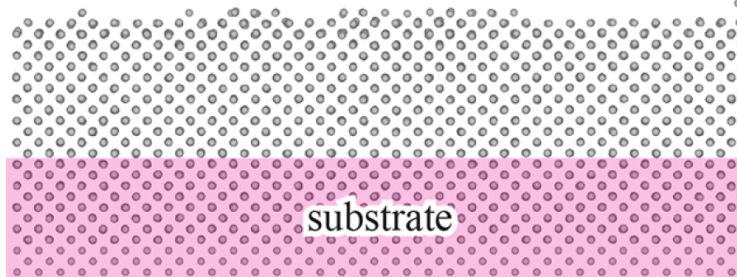
Volume 39 | Issues 29–30 | 2018
Included in this print edition:
Issue 29 (November 5, 2018)
Issue 30 (November 15, 2018)

Journal of
**COMPUTATIONAL
CHEMISTRY**
Organic • Inorganic • Physical
Biological • Materials

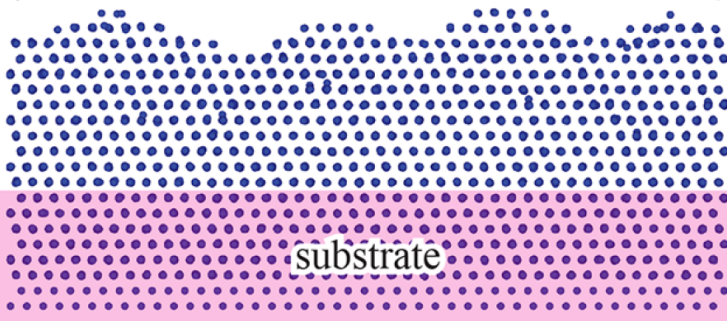


Stability of Structures

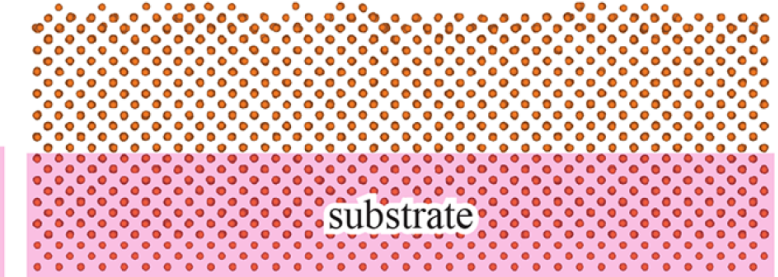
(a) Fe on bcc Fe, atom map



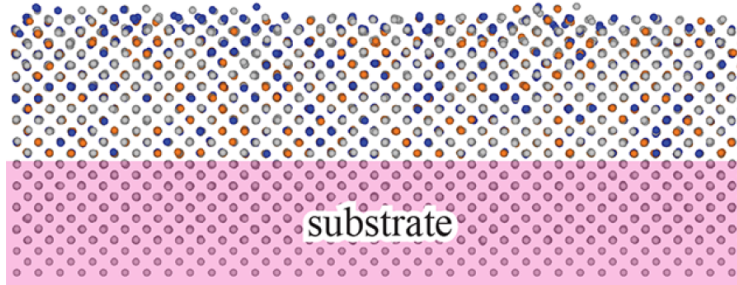
(b) Ni on fcc Ni, atom map



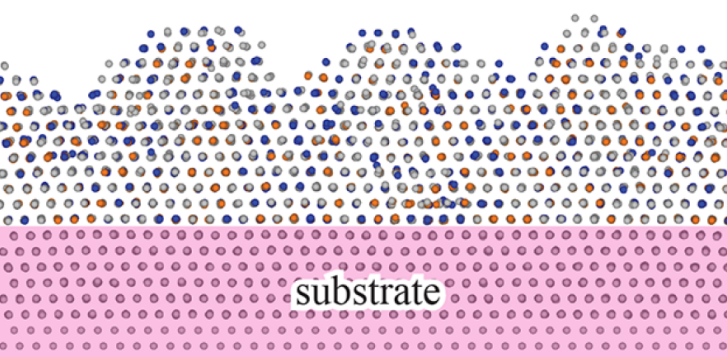
(c) Cr on bcc Cr, atom map



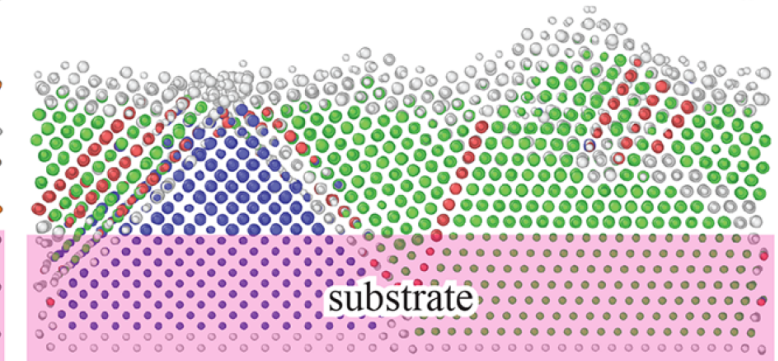
(d) $\text{Fe}_{0.6}\text{Ni}_{0.2}\text{Cr}_{0.2}$ bcc Fe, atom map



(e) $\text{Fe}_{0.6}\text{Ni}_{0.2}\text{Cr}_{0.2}$ on fcc Fe, atom map



(f) $\text{Fe}_{0.6}\text{Ni}_{0.2}\text{Cr}_{0.2}$ on fcc+bcc Fe, structure map



atom: ● Fe ● Cr ● Ni

structure: ● fcc ● bcc ● hcp ● undefined

bcc: x [100], y [010], z: [001] fcc: x [112], y [111], z [110]

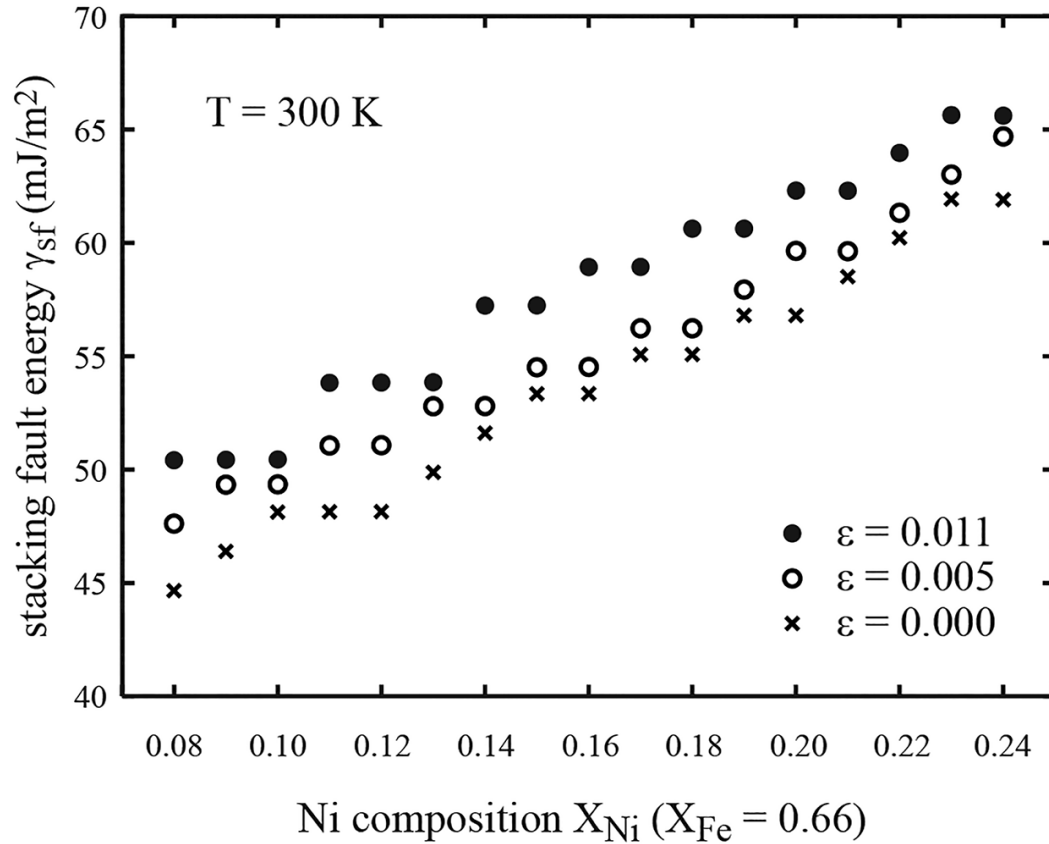
T = 300 K, E_i = 0.1 eV, R ~ 0.5 nm/ns

1 nm

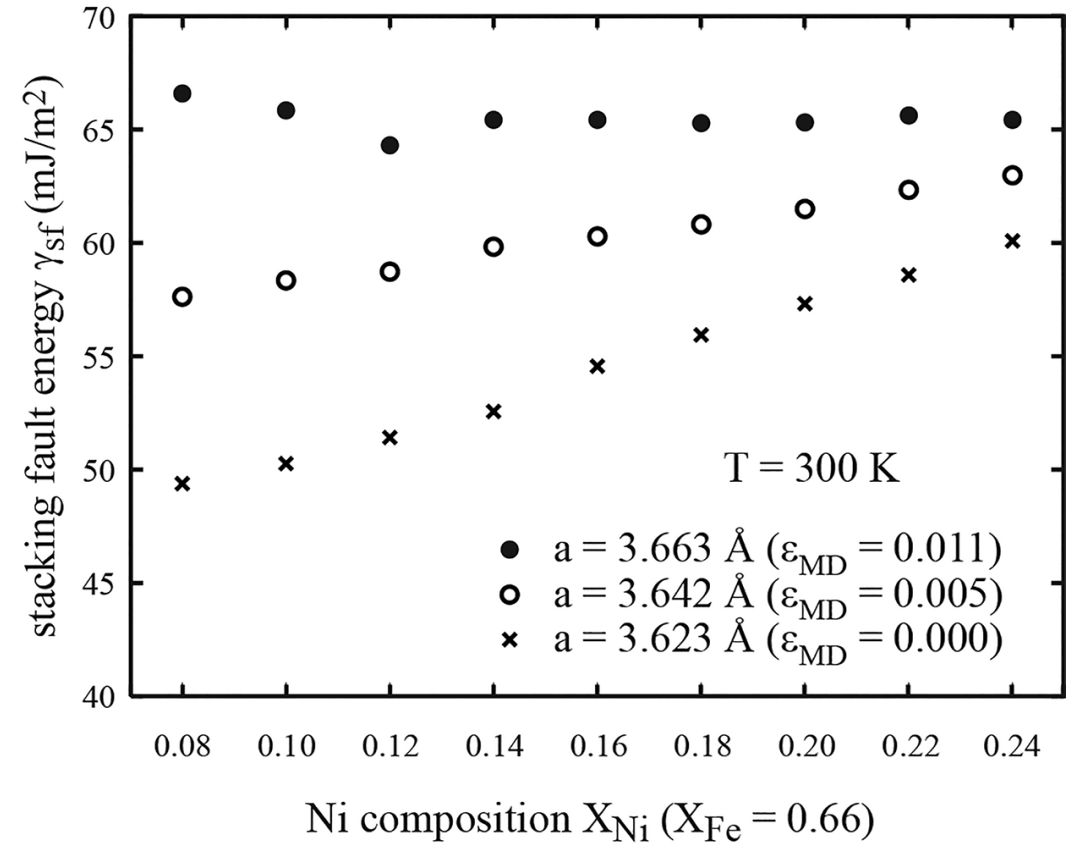
Stability is tested using the most stringent growth simulations.

Stacking Fault Energy

From Potential

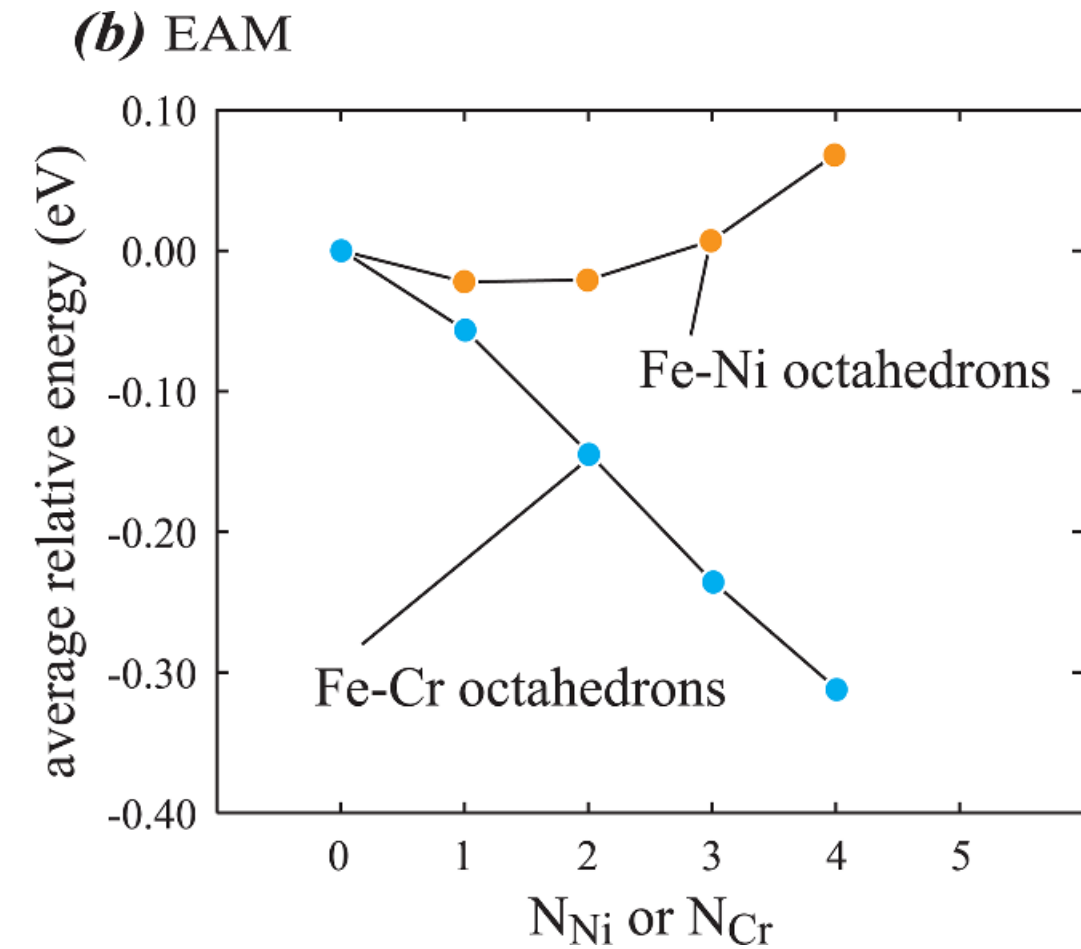
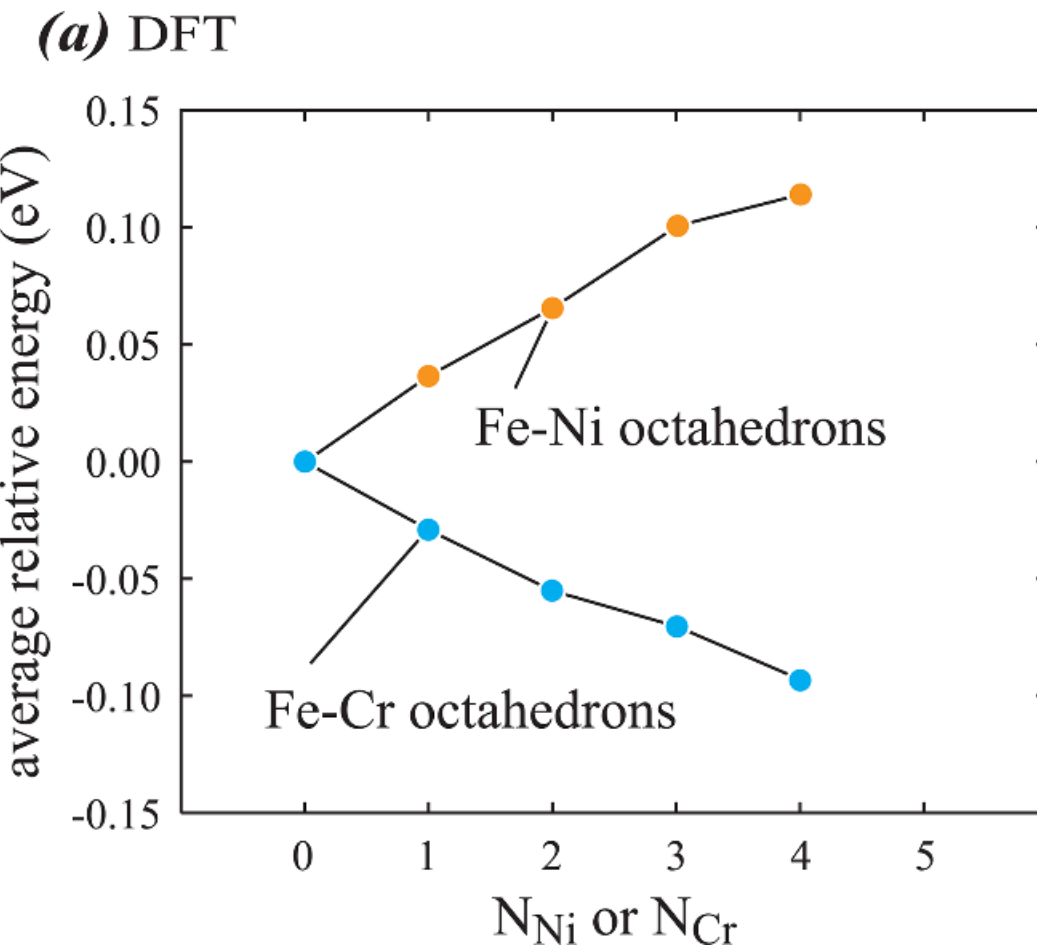


From DFT



Positive slope of SFE with Ni composition is achieved.

H-Metal Interaction Energies

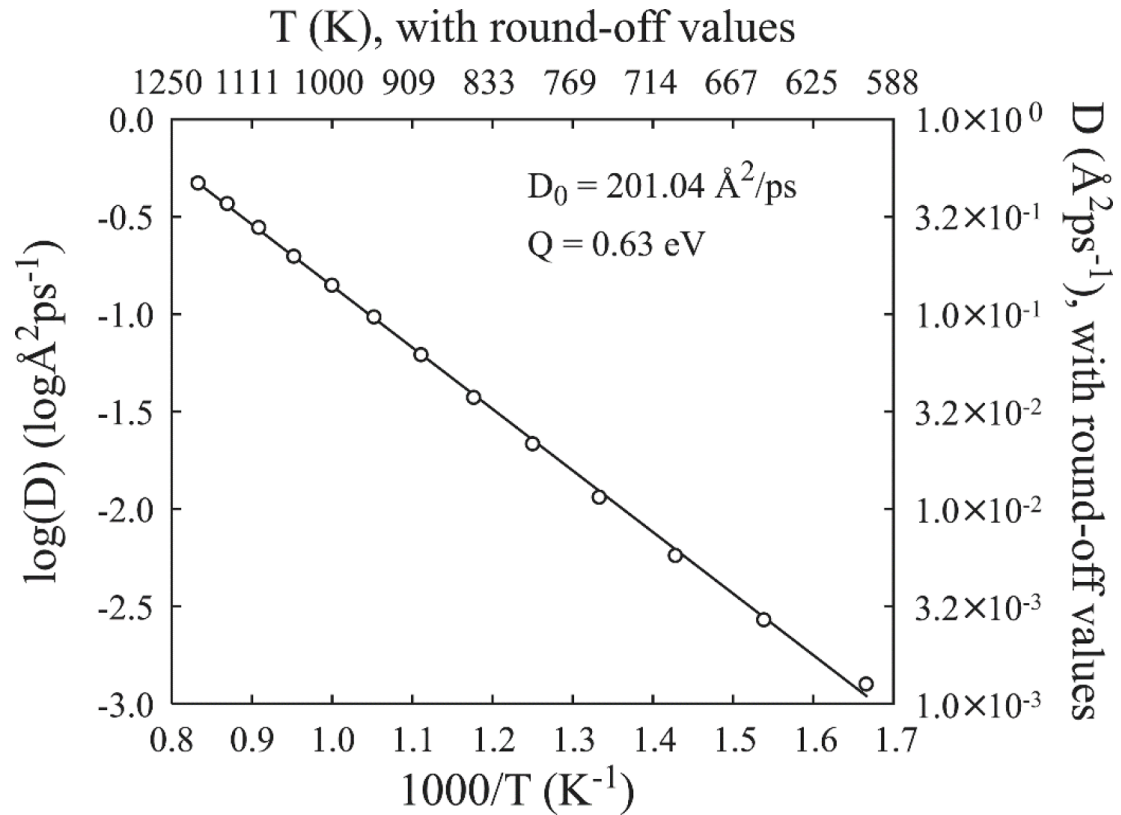


Capture DFT trends that Cr attracts H and Ni repels H.

Statistically-Averaged Diffusivities

$$\left\{ \begin{array}{l} MSD_{1D}(k\Delta t) = \frac{\sum_{i=1}^N \sum_{j=0}^{m-k} [\Delta \alpha_{i,j}^2(k\Delta t)]}{N(m+1-k)} \\ MSD_{2D}(k\Delta t) = \frac{\sum_{i=1}^N \sum_{j=0}^{m-k} [\Delta \alpha_{i,j}^2(k\Delta t) + \Delta \beta_{i,j}^2(k\Delta t)]}{N(m+1-k)} \\ MSD_{3D}(k\Delta t) = \frac{\sum_{i=1}^N \sum_{j=0}^{m-k} [\Delta x_{i,j}^2(k\Delta t) + \Delta y_{i,j}^2(k\Delta t) + \Delta z_{i,j}^2(k\Delta t)]}{N(m+1-k)} \end{array} \right.$$

$$\left\{ \begin{array}{l} D_{1D} = \frac{1}{2} \frac{dMSD_{1D}(t)}{dt} \bigg|_{t \rightarrow 0} \\ D_{2D} = \frac{1}{4} \frac{dMSD_{2D}(t)}{dt} \bigg|_{t \rightarrow 0} \\ D_{3D} = \frac{1}{6} \frac{dMSD_{3D}(t)}{dt} \bigg|_{t \rightarrow 0} \end{array} \right.$$

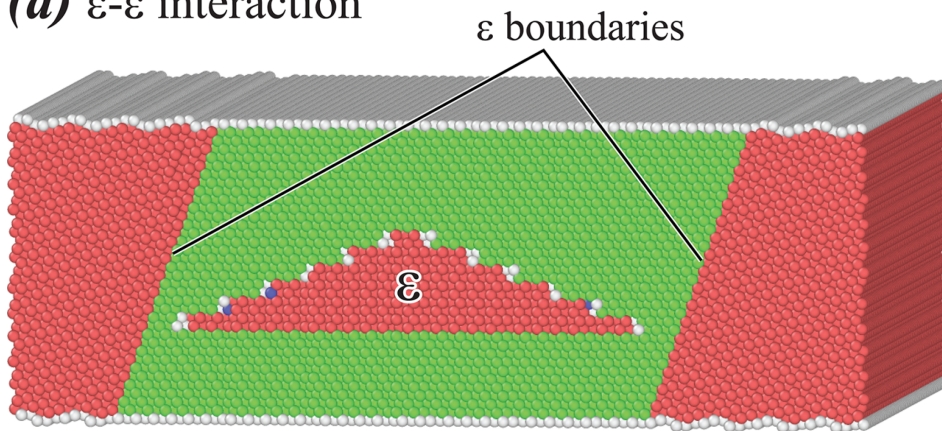


- MD accounts for statistics of alloys.
- Calculated barrier 0.63 eV agrees well with the measured 0.51 eV: San Marchi et al, Inter. J. Hydro. Ener., 32, 100 (2007).

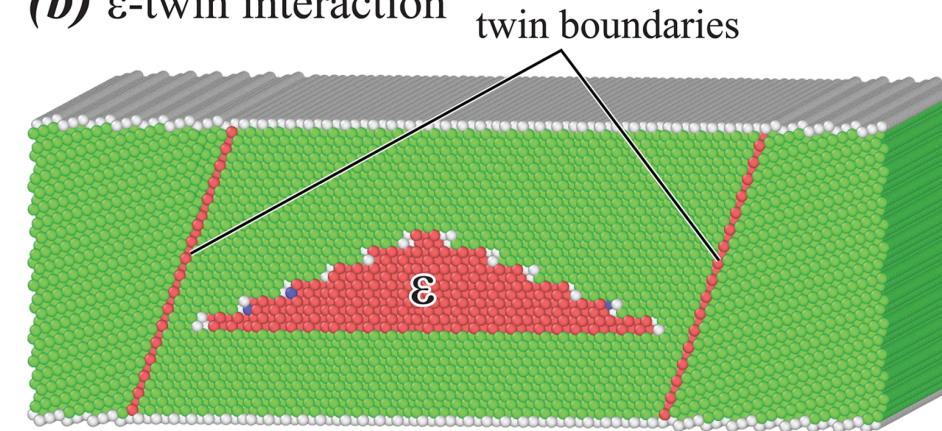
Experimental Validation: Slip Band Collision

Simulations

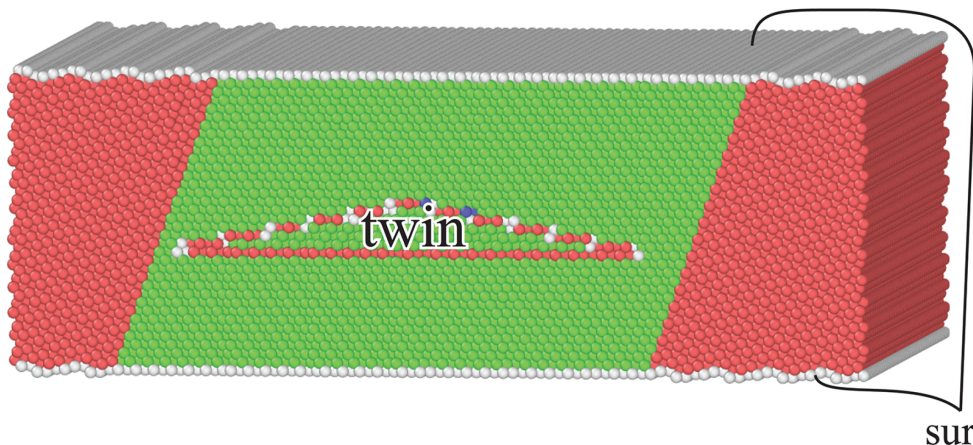
(a) ϵ - ϵ interaction



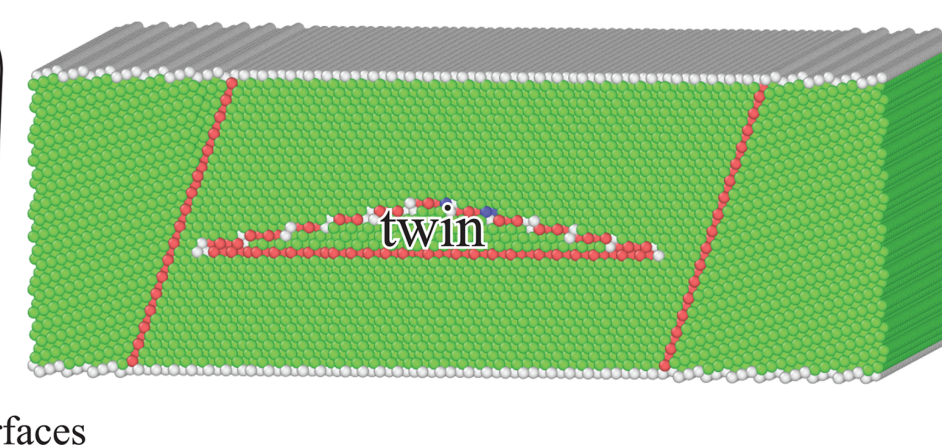
(b) ϵ -twin interaction



(c) twin- ϵ interaction



(d) twin-twin interaction



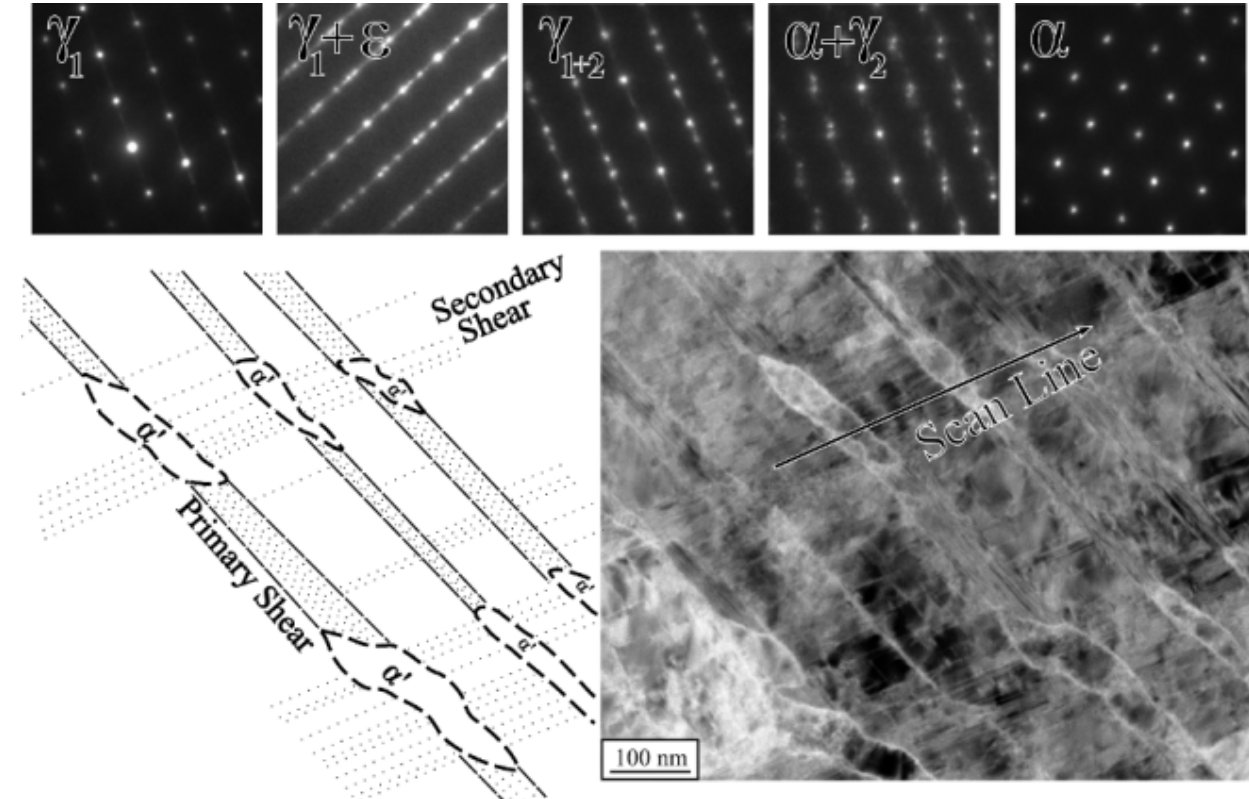
Experimentally, the material deforms through formation and extension of slip bands.

Simulations of slip band collision provide a good problem to validate our potential.

Slip band collision occurs when a shear stress is applied to the surfaces in our MD model.

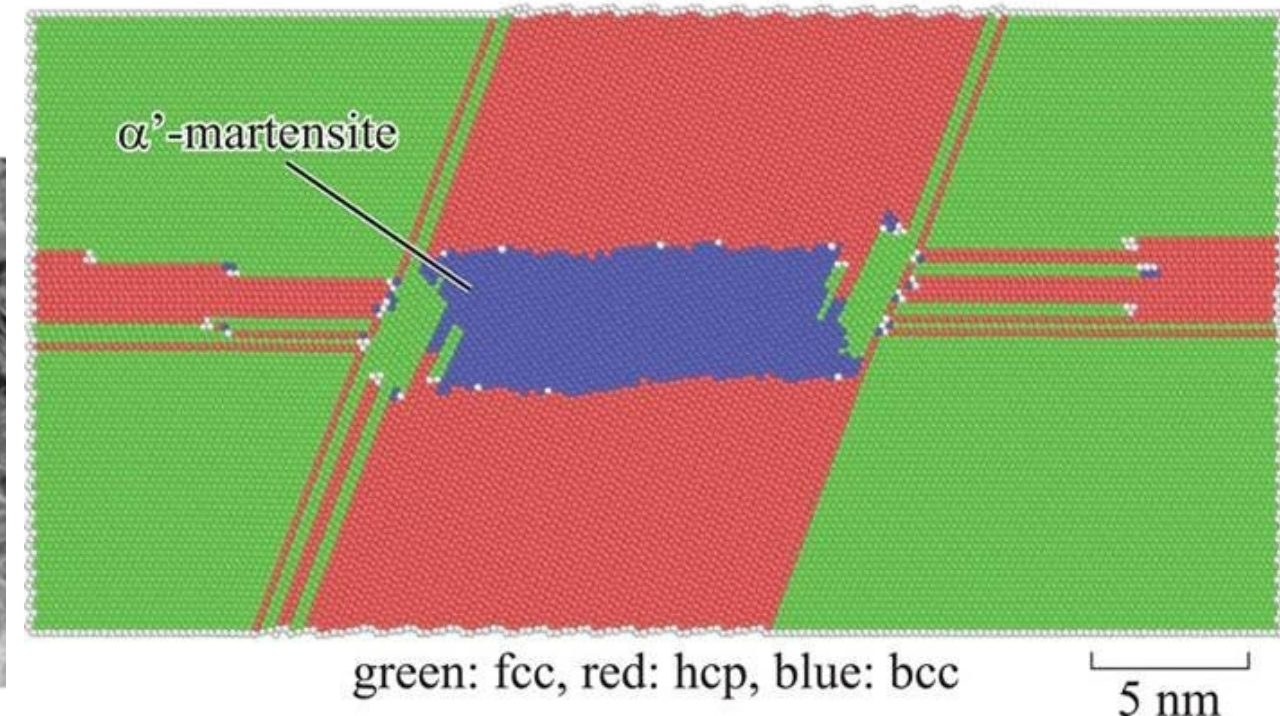
Validation: α' Martensite Formation

Transmission electron microscope (TEM)
from Doug Medlin



Molecular dynamics (MD)

collision of an ε -martensite band (screw Burgers vector)
with an ε -martensite band at $\tau = 1.15$ GPa

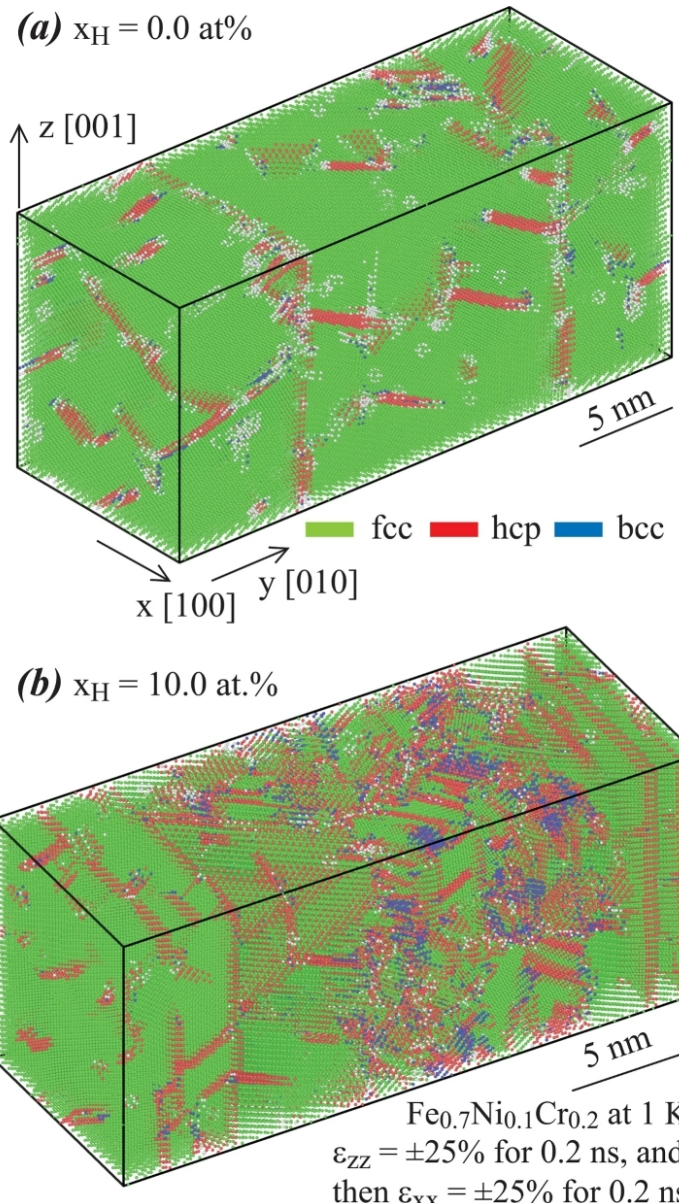


Both TEM and MD show:

$\{111\}_\gamma // \{0001\}_\varepsilon // \{011\}_{\alpha'}$
 $\langle 110 \rangle_\gamma // \langle 11\bar{2}0 \rangle_\varepsilon // \langle 111 \rangle_{\alpha'}$

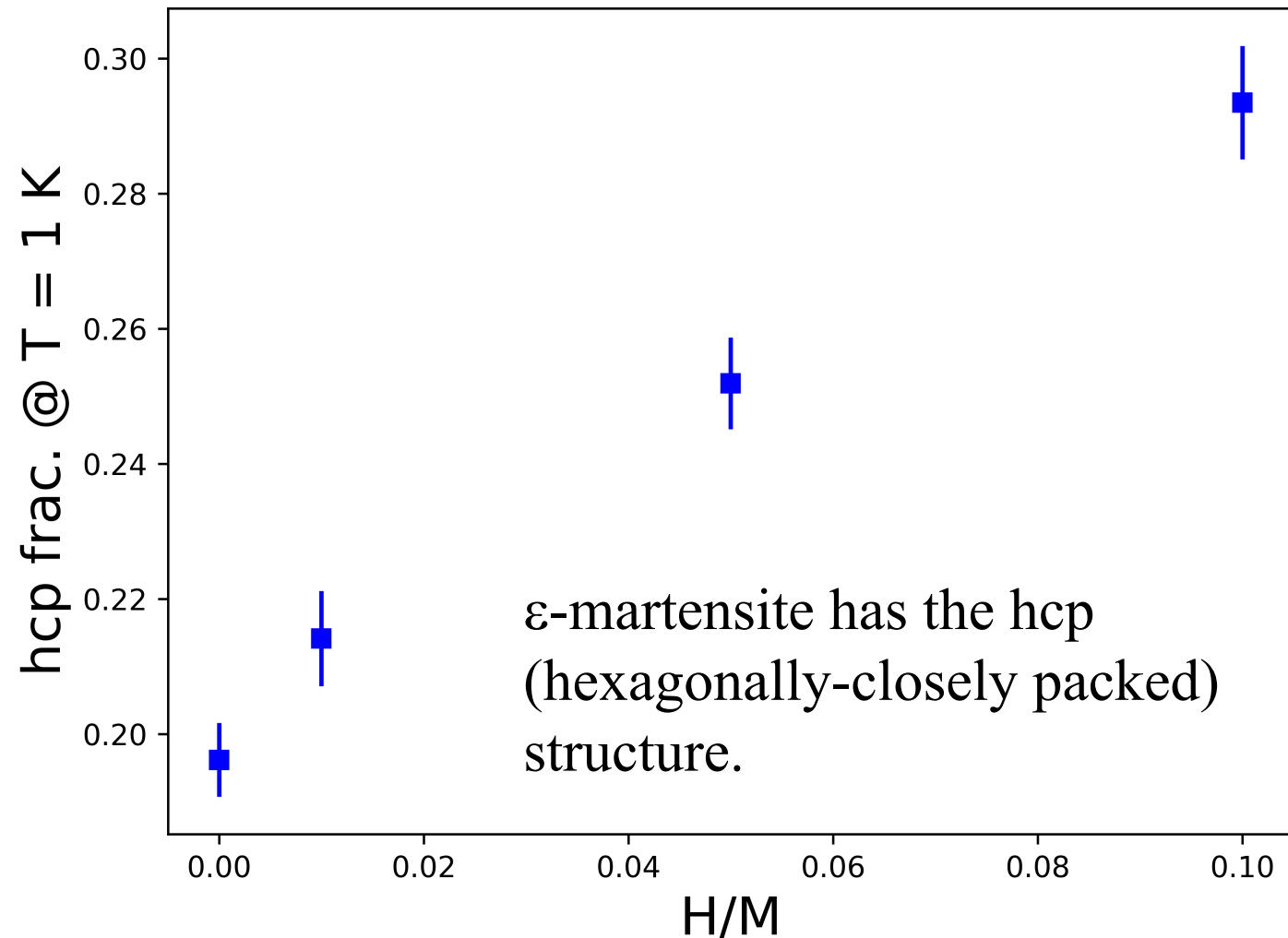
Validation: H promotes ε -Martensite Slip

MD configurations



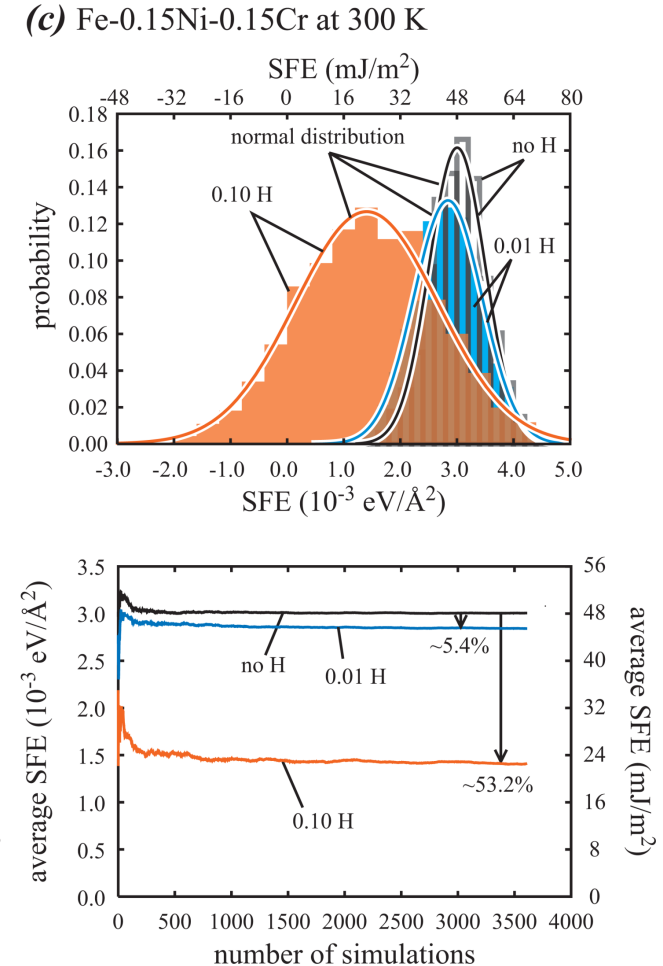
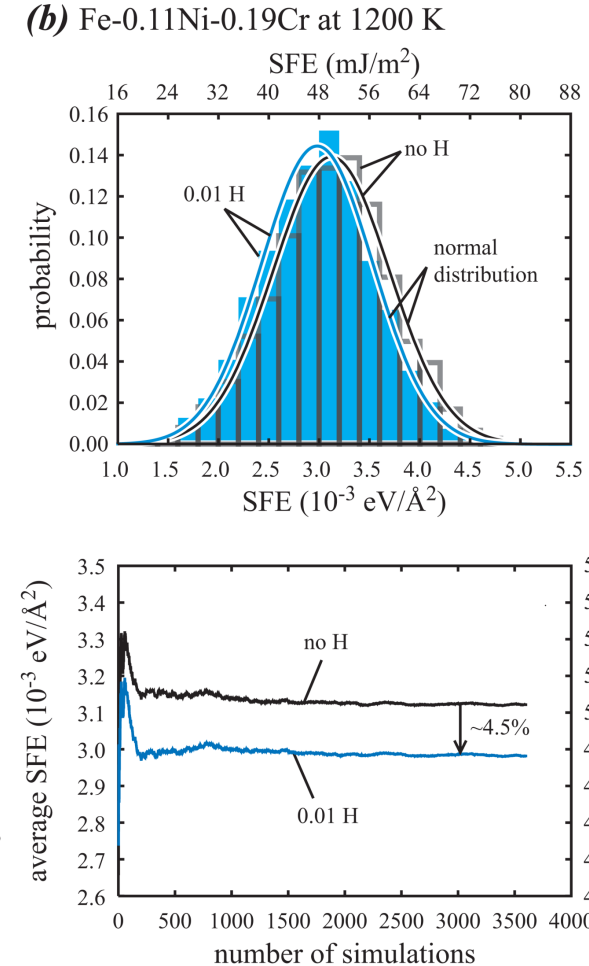
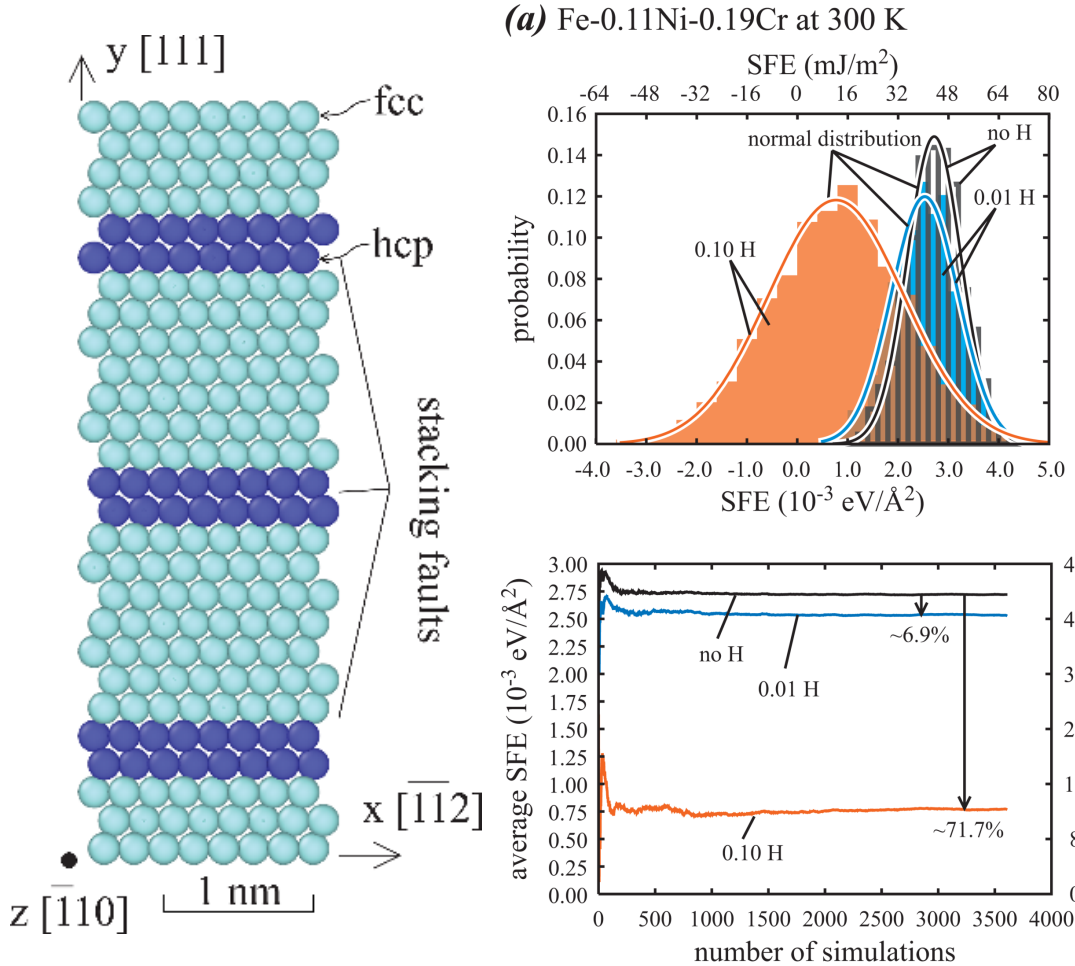
MD predicted Band

ε -martensite fraction vs. H content



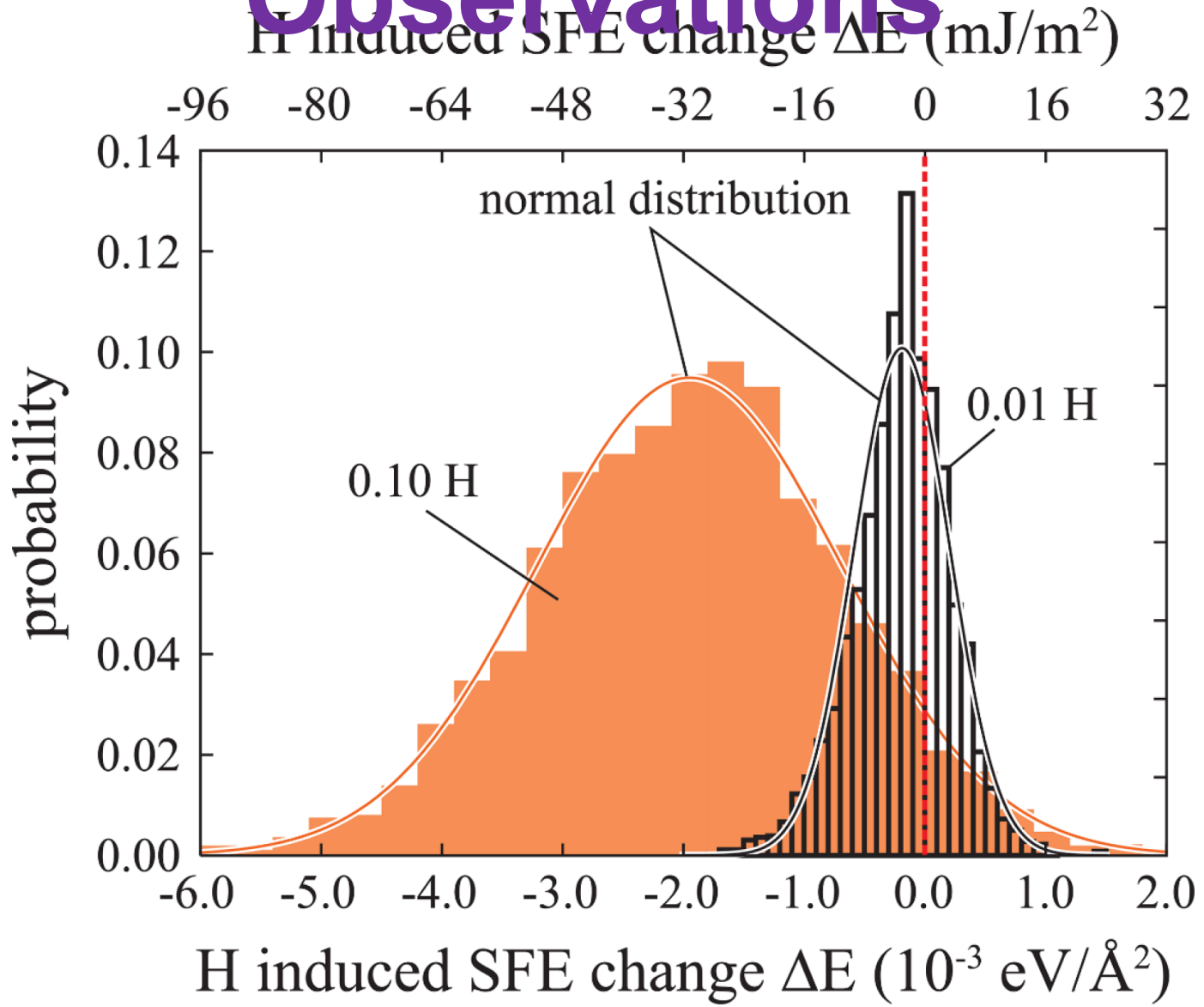
Experiments indicate that H promotes ε -martensite slip bands, Metall. Mater. Trans. A, 52, 1516 (2021).

SFE Distributions from 57600 MD Simulations

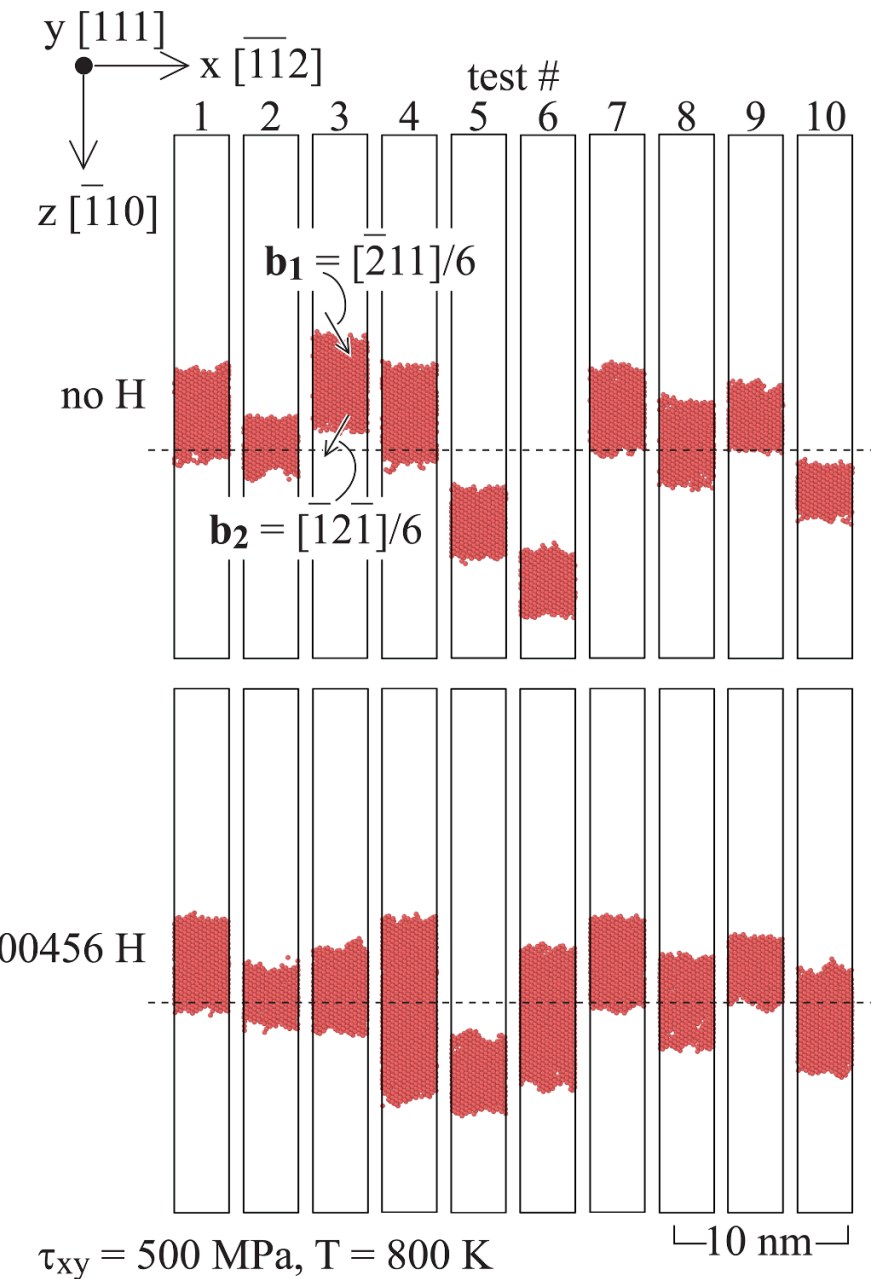


Stacking fault energy based alloy screening for hydrogen compatibility: Gibbs et al., JOM, 72, 1982 (2020).

Additional Observations



After 1.8 ns MD simulations

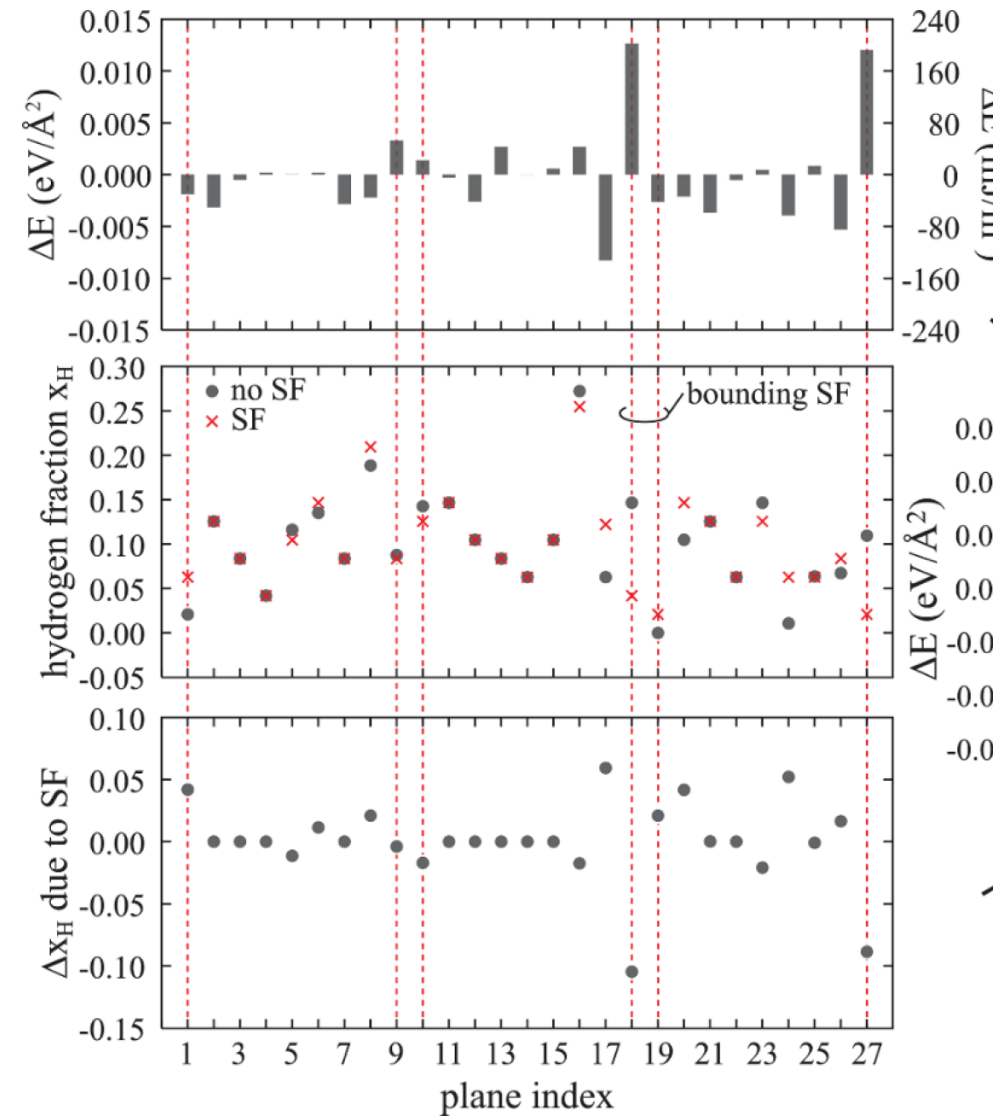
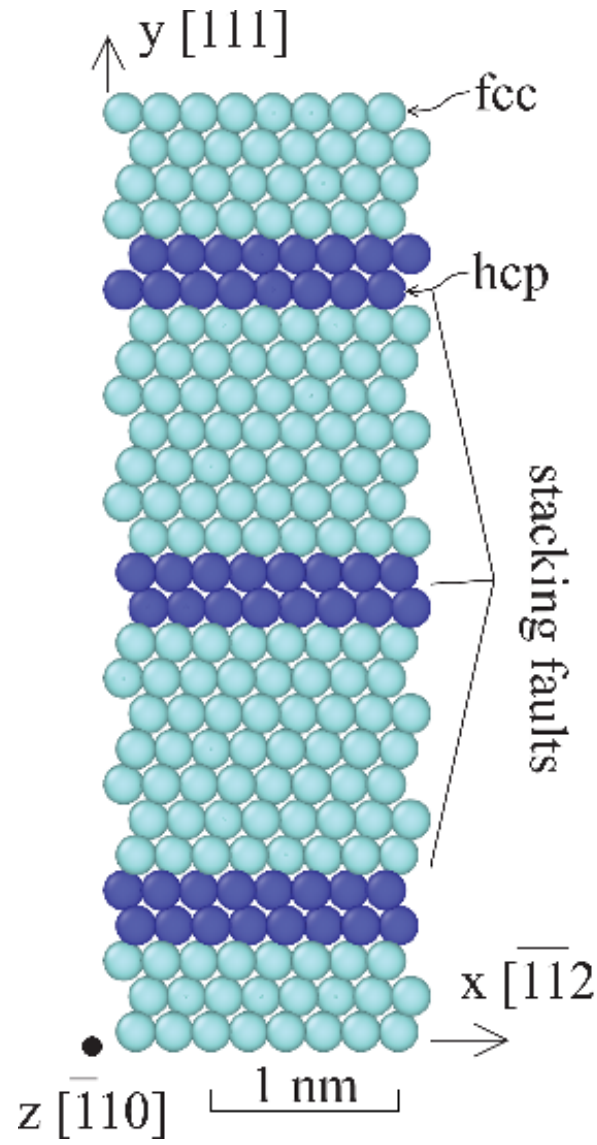


SUMMARY

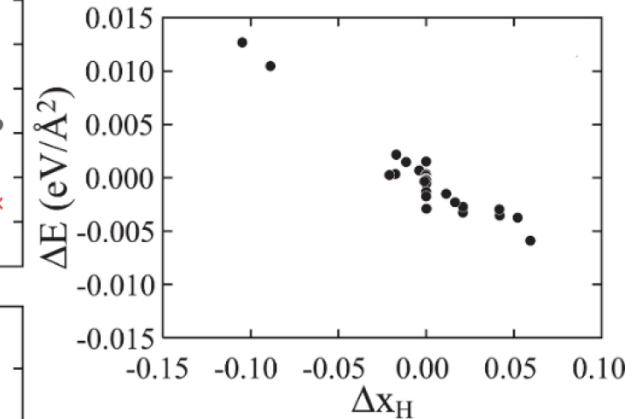
1. An Fe-Ni-Cr-H potential suitable for studying SFE and the related slip bands has been developed.
2. This potential reproduces the experimentally observed H effects on ε - and α' - martensite formation in slip bands.
3. SFE in stainless steels is not a single value, but rather is a distribution due to local composition variations.
4. Hydrogen significantly reduces the mean SFE, in agreement with experiments.
5. Previous views on SFE effects are too simplistic.

Spare Slides

Plane-Resolved Energies



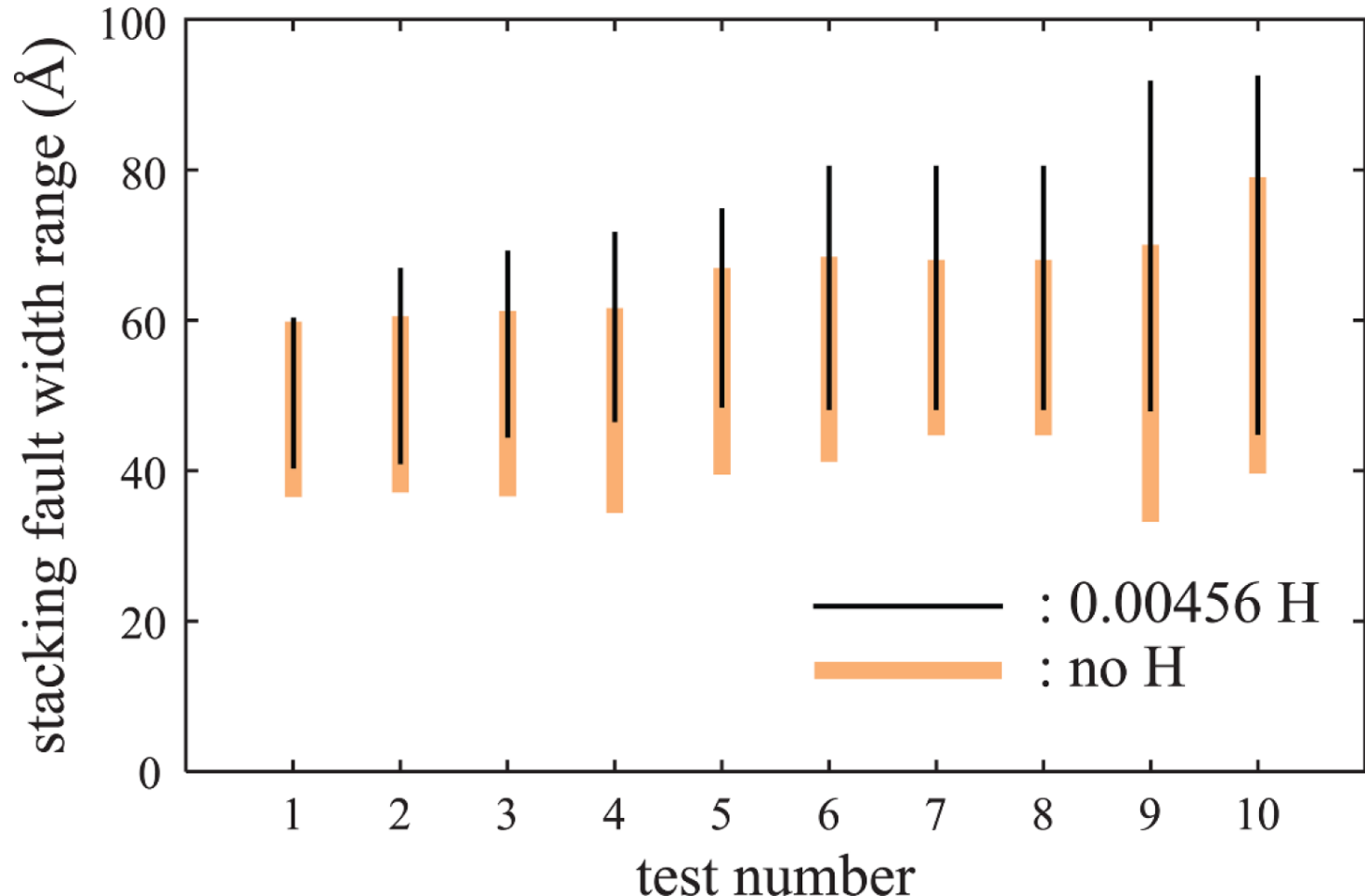
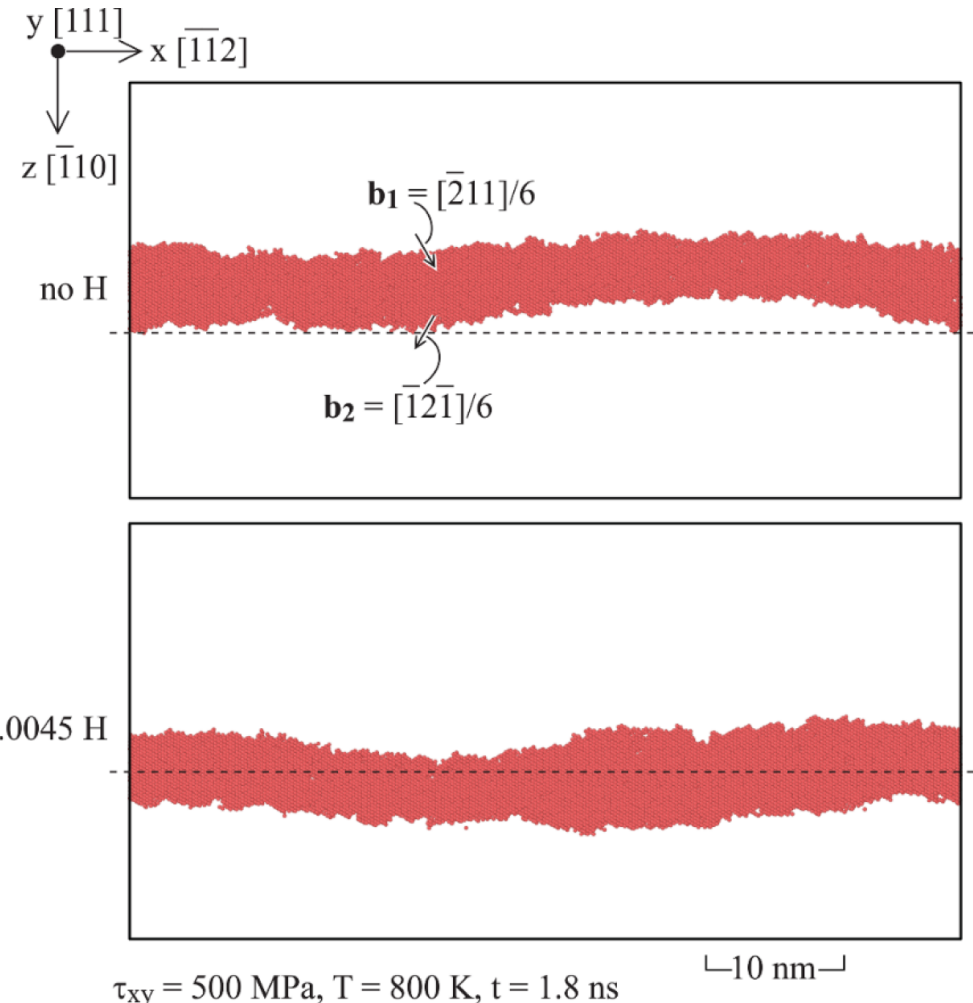
MD for 5.5 ns
(average time
5 ns)



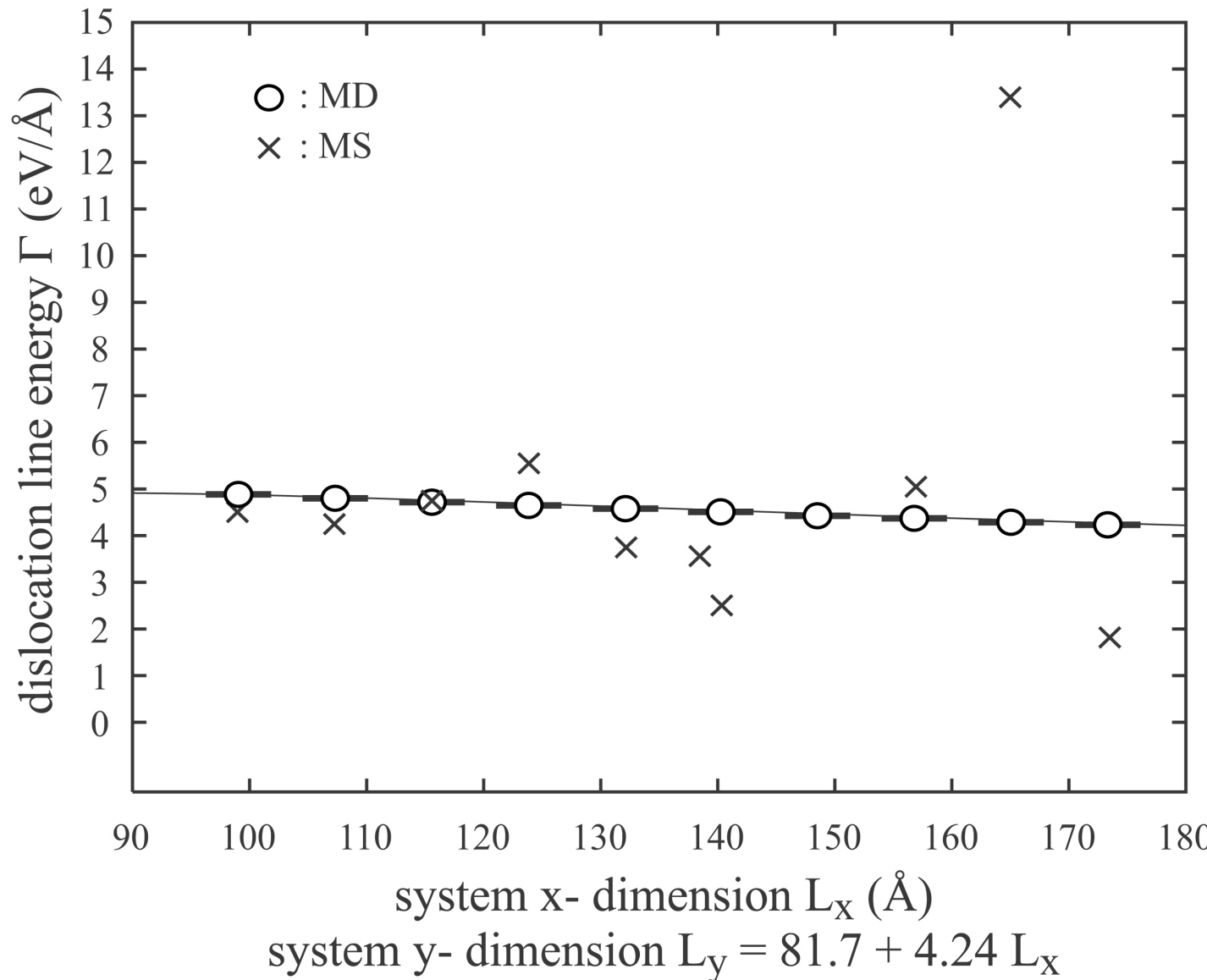
Stacking Fault Width of Long Dislocations

H effects on MD configurations

Stacking fault width range from 10 replicas



Errors of (Time-Averaged) MD vs. MS



1. X. W. Zhou, and M. E. Foster, *Phys. Chem. Chem. Phys.*, 2021, 23, 3290.
2. X. W. Zhou, D. K. Ward, J. A. Zimmerman, J. L. Cruz-Campa, D. Zubia, J. E. Martin, and F. van Swol, *J. Mech. Phys. Solids*, 2016, 91, 265.